Inheritance of the epigenetic signature and reduced intermuscular bone phenotype acquired via DNA methylation editing of the *runx2b* promoter in zebrafish

Fang Liang[1,2,#], Biyu Wu[1,#], Jiayi Liu[1], Xue Wang[1], Minxing Liang[1], Chaoyi Wang[1], Jingyi Zhang [1], Junjie Wang[1,2], Yutao Miao[1,2], Kangsen Mai[1,3], Jun Zhao[1,*], Xuegeng Wang[1,2,*]

[1] Institute of Modern Aquaculture Science and Engineering, Guangdong-Macao Joint Laboratory for Aquaculture Breeding Development and Innovation, School of Life Sciences, South China Normal University, Guangzhou 510631, China

[2] Guangdong Provincial Key Laboratory of Insect Developmental Biology and Applied Technology, School of Life Sciences, South China Normal University, Guangzhou, 510631, China

[3] Fisheries College, Ocean University of China, Qingdao, 266003, China

[#] Authors contributed equally to this work.

[*] Corresponding authors: Z. J. (Email: zhaojun@scnu.edu.cn); X.W. (Email: wangxuegeng@scnu.edu.cn)

ABSTRACT

The presence of intermuscular bones (IBs) can directly affect the economic value of aquaculture fish. Although genome editing can create IB-free fish by knocking out key IB-related genes, such as *runx2b*, the associated DNA sequence alterations raise food safety and health concerns, limiting its breeding applications. In this study, we used the CRISPR/dCas9 mediated epigenome-editing technology targeting the *runx2b* promoter in zebrafish to alter DNA methylation patterns without changing the DNA sequence. Our results showed that higher *runx2b* promoter methylation patterns significantly inhibited *eGFP* mRNA expression levels in the recombinant plasmid. Using the CRISPR/dCas9-Dnmt7 system to enhance methylation of the zebrafish *runx2b* promoter, we observed a significant decrease in *runx2b* mRNA expression levels in the F0 generation. The IBs in the 11th - 16th muscle segments of the adult F0 fish were significantly shorter compared with the controls. Inbreeding of fish was used to produce F1 and F2 offspring that retained these high promoter methylation levels, along with the persistent runx2b expression suppression and IB development inhibition. Transcriptome sequencing analysis suggested that increasing *runx2b*

Science Press ZR Zoological Research

promoter methylation levels may synergistically induce additional epigenetic modifications, potentially affecting the PPAR signaling pathway and FoxO transcription factor regulation, which appears to inhibit osteoblast proliferation and differentiation. Overall, this study demonstrates an innovative application of epigenetic editing technology for aquaculture breeding. By precisely regulating the expression patterns of key genes for economically important traits while preserving genomic DNA integrity, this approach provides a theoretical foundation and technical support for improving fish economic traits.

Keywords: CRISPR/dCas9; *runx2b*; DNA Methylation; Intermuscular Bone; Zebrafish

INTRODUCTION

Intermuscular bones (IBs), small hard bones embedded within fish myosepta, are classified into three types by their attachment location on the fish body: epineural bones on the dorsal side, epicentral bones in the middle, and epipleural bones on the abdominal side (Danos & Ward, 2012). IB characteristics being difficult to remove negatively impact consumer acceptance and economic value in aquaculture because of processing difficulties and potential health hazards to the throat or digestive organs (Erik, 2020). Consequently, breeding IB-free strains has practical significance for the aquaculture industry, aiming to enhance product value and safety.

Over the past decade, extensive research has focused on elucidating the molecular mechanisms underlying IB development in fish by conducting genetic selection to breed new strains with few or no IBs. Traditional efforts to reduce IBs via genetic selection have recently been augmented by CRISPR/Cas9-mediated knockout of key genes, such as *runx2b* and *bmp6*, resulting in the successful generation of IB-free strains in zebrafish (Nie et al., 2022; Xu et al., 2022), blunt snout bream (*Megalobrama amblycephala*) (Dong et al., 2023), and crucian carp (*Carassius auratus*) (Gan et al., 2023; Kuang et al., 2023). This method offers an efficient strategy for directed genetic improvement in aquaculture. However, while effective, this strategy relies on permanent DNA sequence alterations, raising unresolved biosafety and ecological concerns that hinder commercial adoption and regulatory approval (Okoli et al., 2022; Wang et al., 2024). Therefore, novel genetic

Science Press ZR Zoological Research

breeding frameworks that enable the precise regulation of key economic trait genes without altering genomic DNA sequences are urgently needed to overcome the inherent limitations of transgenic and genome-editing approaches in aquatic animal breeding research.

Epigenetic modifications, including DNA methylation, histone modifications, and non-coding RNA-mediated regulation, offer a promising alternative to modulate gene expression patterns without altering DNA sequences (Allis & Jenuwein, 2016; Harvey et al., 2018). As the most extensively studied epigenetic modification, DNA methylation, catalyzed by methyltransferases (DNMTs), dynamically regulates chromatin structure and transcriptional activity (Jin et al., 2011; Zhong et al., 2021), thereby driving phenotypic trait differentiation (Nilsson et al., 2021; Podgorniak et al., 2022). To harness such mechanisms, CRISPR/catalytically dead Cas9 (dCas9) systems facilitate targeted epigenetic editing by fusing dCas9 to effector domains, such as DNMTs and TETs (Liu et al., 2018; Park et al., 2022), thereby enabling reversible, sequence-preserving gene regulation (Sadakierska-Chudy et al., 2015). Notably, recent studies have shown that epigenetic marks and their associated phenotypes induced by DNA methylation editing undergo stable transgenerational inheritance in mice (Yuta et al., 2023).

We have focused on *runx2b*, a key regulatory gene governing IB development through controlling mesenchymal stem cell differentiation into osteoblast precursors *in vivo* and driving osteoblast-to-osteocyte transformation via multiple signaling pathways (Flores et al., 2004). Knocking out this gene completely ablates IBs, while preserving core muscle nutrient profiles, including most amino acids and fatty acids (Nie et al., 2022). Importantly, *runx*2 (homologous to zebrafish *runx2b*) expression levels are negatively correlated with the methylation level of CpG sites in the distal P1 promoter in human osteoarthritis chondrocytes (Takahashi et al., 2017). These findings suggest that targeted hypermethylation of the *runx2b* promoter could suppress IB development while preserving genomic integrity.

Building on these insights, our laboratory pioneered a targeted DNA methylation editing system by fusing dCas9 with the catalytic domains of Dnmt7 and Tet2 from zebrafish for site-specific methylation and demethylation in the zebrafish genome (Liang et al., 2023a). In this study, we demonstrated that CRISPR/dCas9-Dnmt7 mediated methylation of the *runx2b* promoter can reduce

Science Press ZR Zoological Research

IBs in zebrafish. We further evaluated the inheritance of the edited epigenetic marks and decoded the molecular cascade links among epigenetic modifications, gene expression, and phenotypic traits, which can be used to generate IB-reduced fish through non-GMO strategies. Theoretically, this work advances aquatic breeding theory by elucidating the epigenetic regulation of development. Practically, it establishes core technologies for trait-directed aquatic animals in breeding, with the ultimate goal of producing premium aquaculture products while preserving genomic integrity.

MATERIALS AND METHODS

Zebrafish maintenance

All zebrafish (AB strain, wild-type) used in this study were raised in the zebrafish facility at South China Normal University. The protocol was approved by the Animal Care and Use Committee of South China Normal University (approval number: SCNU-SLS-2021-026). The fish facility was equipped with a standard recirculating water system, maintaining a 14-/10-hour light/dark photocycle and water temperature of 28 ± 1°C. The fish were fed newly hatched brine shrimp twice daily, and all other husbandry conditions and procedures were conducted in accordance with relevant international regulations.

Plasmid construction

To construct the pCS2^{+}-prunx2b-eGFP recombinant plasmid, the pCS2^{+}-eGFP backbone was linearized by *Sal*I/*Hind*III double digestion to remove the CMV IE94 promoter, followed by purification of the digested vector. The *runx2b* gene location information was obtained from the Ensembl database (https://asia.ensembl.org/Danio_rerio/Info/Index), with a ~1500 bp upstream sequence rich in CpG sites predicted to be the promoter region. This promoter fragment was amplified from 48 hours post-fertilization (hpf) genomic DNA using primers containing *Sal*I/*Hind*III restriction sites (F: 5′-ACGCGTCGACTGTATTGTTTAAAACCTGCCCC-3′; R: 5′-CCCAAGCTTGCCACTTTCGCTCCCAAATT-3′). The PCR product was purified, ligated into the pMD™19-T simple vector (TaKaRa, Japan), and sequence-verified by Sanger sequencing. The recombinant plasmid was then digested with *Sal*I/*Hind*III to harvest the *runx2b* promoter fragment with sticky ends, which was subsequently ligated into the linearized pCS2^{+}-eGFP backbone.

Science Press ZR Zoological Research

Single guide RNA (sgRNA) production

Two sgRNAs were designed based on the location of PAM sequences for DNA methylation editing strain construction, both of which were located in the *runx2b* promoter region. A third sgRNA was designed to construct a knockout strains targeting the second exon of *runx2b*. All target sites were evaluated with CRISPOR (Concordet & Haeussler, 2018) to confirm that no off-target site were identified with mismatches of less than 5. All sgRNAs used in this study were synthesized by Qingke Biotechnology Co., Ltd. (Beijing, China). The sgRNA sequences are shown in Table S1.

mRNA synthesis and microinjection

The dCas9-Dnmt7 mRNA was *in vitro* transcribed from linearized pT3TS-dCas9-Dnmt7 plasmid templates (Supplementary Figure S1) using the T3 mMESSAGE mMACHINE® Kit (Invitrogen, USA) and purified using the RNeasy® Mini Kit (QIAGEN, Germany). For the DNA methylation editing strain (F0), one-cell stage zebrafish embryos were injected with 2 nL of a mixture containing dCas9-Dnmt7 mRNA (400 ng/μL) and sgRNA (200 ng/μL). The uninjected wild-type zebrafish was used as the control group (F0). The F1 generation was obtained by inbreeding the F0 adults. And the F2 generation was inbred by the F1 generation.

For the gene knockout strain (F0), embryos were injected with 2 nL of a complex (5 μM) containing Cas9 protein (NEB, USA) and sgRNA. Injected founders (F0) were outcrossed to AB to obtain F1. F1 fin clips were genotyped by PCR using the primers flanking the target site to identify frameshift alleles. The primer pair used for genotyping is: *runx2b*-fwd: 5'-CGGTGTCGGTGAAGATGAAT -3' and *runx2b*-rev: 5'- ACGCAACAGGTAGCGTTTTA -3'. Heterozygous F1 were incrossed to establish F2 for experiments.

Real-time quantitative PCR (RT-qPCR)

The TRNzol reagent (TIANGEN, China) was used to extract total RNA. RNA concentrations were quantified using the NanoDrop One (Thermo Fisher Scientific, USA). cDNA was synthesized using a StarScript Pro All-in-one RT Mix with gDNA Remover kit (GenStar, China) for RT-qPCR. RT-qPCR analysis was performed on a CFX96 real-time PCR system (Bio-Rad, USA) using Hieff™ qPCR SYBR® Green Master Mix (Yeasen Biotech, China). Experiments were conducted in triplicate with 30 embryos or five tissue samples per replicate. Zebrafish *gapdh* served as the reference gene,

Science Press ZR Zoological Research

and data were analyzed using the $2^{-\Delta\Delta Ct}$ method. The relevant primer sequences are listed in Table S2.

Multiplex Bisulfite Sequencing PCR (BSP)

At 48 hpf, injected embryos were collected for genomic DNA extraction using a genome DNA extraction kit. Total DNA was extracted from three pools of ten randomly collected embryos. The EZ DNA Methylation-Lightning™ kit (Zymo Research, USA) was used to perform bisulfite treatment on plasmids or DNA, converting unmethylated cytosines (C) to uracil (U), while methylated cytosines remained unchanged. For the detection of plasmids, specific BSP primers (Table S3) were designed to amplify the CpG island region of the *runx2b* promoter. Bisulfite-treated DNA was amplified using BSP primers (Table S4). Multiplex BSP integrates multiplex PCR and methylation-specific high-throughput sequencing to simultaneously detect methylation levels across multiple gene regions. Sequencing was performed by MethylGene Tech Co., Ltd. (Guangzhou, China). High-quality reads were aligned to the reference genome (GRCz11) for CpG methylation quantification.

Whole-mount in situ hybridization (WISH)

The coding sequence of zebrafish *runx2b* was cloned into the T-zero vector using primers runx2b-probeF (5'-TCTAGAATTCACAAACCCACCGCAAG-3') and runx2b-probeR (5'-TAATACGACTCACTATACACTCCTCCACTTCCGTCAG-3'), which incorporated a flanking *Xba*I restriction site and T7 promoter. Linearized plasmid templates were then used to synthesize Digoxigenin-labeled antisense RNA probes using T7 RNA polymerase (TaKaRa, Japan) and DIG RNA labeling mixture (Roche, USA). Whole-mount ISH was performed on 48 hpf larvae following established protocols (Chitramuthu & Bennett, 2013; Thisse & Thisse, 2008). Finally, the specimens were mounted in glycerol and imaged using a stereomicroscope (SZ-0850T, AOSVI, China) equipped with a digital CCD camera.

Transcriptome analysis

Total RNA was extracted from 40 dpf (days post-fertilization) zebrafish caudal peduncles using TRNzol reagent. Total RNA was extracted from three pools of five randomly collected caudal peduncles. Samples were submitted to IGE Biotech Co., Ltd. (Guangzhou, China) for RNA

Science Press ZR Zoological Research

sequencing (RNA-seq). The transcriptome analysis procedures were performed as previously described (Li et al., 2024; Liang et al., 2023b). Briefly, RNA integrity was verified using an Agilent 2100 Bioanalyzer (Agilent Technologies, USA). Subsequently, mRNA was enriched using mRNA Capture Beads, fragmented, reverse transcribed into cDNA, and purified with DNA Clean Beads. The purified cDNA was subjected to end repair, A-tailing, and ligation to Illumina adapters. The ligated products were PCR-amplified, purified using DNA Clean Beads, and sequenced on an Illumina PE150 (Pair-end 150 bp) platform. Finally, the sequencing data were filtered using fastp (v.0.23.4)(Chen et al., 2018) for quality control, yielding clean reads. The clean reads were mapped to the reference genome (ASM2018471v1) using Hisat2 (Kim et al., 2015), to calculate the expression level of each gene. Statistically significantly differentially expressed genes (DEGs) were identified using DESeq2 (Love et al., 2014), with functional annotation and enrichment analysis performed using the Gene Ontology (GO)(Consortium, 2015), and Kyoto Encyclopedia of Genes and Genomes (KEGG) methods.

2.9 Alizarin Red S bone staining

Adult zebrafish skin and scales were dissected with forceps and fixed for ≥ 3 days in either 95% ethanol or 4% paraformaldehyde. Samples underwent pre-transparency in 1% KOH for 2 hours, followed by immersion in an Alizarin Red S staining solution (saturated Alizarin Red S: 0.5% KOH=1:9) for 6 hours. A graded glycerol series was then applied sequentially until the muscle became transparent and the IBs were clearly visible. Processed zebrafish are placed in glycerol for photography. The number of intermuscular bones is counted, and their lengths are measured using ImageJ software.

Statistical analysis

The data are presented as the mean ± SEM (Standard Error of the Mean). Statistical analysis was performed by one-way analysis of variance (ANOVA), with $P < 0.05$ indicating statistical significance.

Science Press ZR Zoological Research

RESULTS

Increased *runx2b* promoter methylation suppressed *runx2b* expression levels

To explore the impact of *runx2b* promoter methylation on gene expression patterns in zebrafish, we replaced the CMV IE94 promoter in the pCS2^{+}-eGFP plasmid with the zebrafish *runx2b* promoter, generating the pCS2^{+}-prunx2b-eGFP plasmid (Figure 1A; Supplementary Figure S2). The plasmid was transformed into DMT competent cells or Trans10 competent cells to produce differentially methylated templates. The amplified fragment's location, which is indicated in Figure 1B, contained a total of 23 CpG sites. The plasmids from DMT cells (D plasmid) showed an average methylation level of 11.3% across these sites, while those from Trans10 cells (T plasmid) exhibited significantly higher methylation at 41.3% (Figure 1C).

Both the D and T plasmids were diluted to 30 ng/μL and microinjected separately into one-cell stage zebrafish embryos. At 48 hpf, *eGFP* mRNA expression levels from the T plasmid were significantly reduced compared with those from the D plasmid (Figure 1D). Quantitative analysis further confirmed a significantly lower relative eGFP fluorescence intensity in T plasmid-injected embryos compared with D plasmid-injected embryos at 48 hpf (Figure 1E). Fluorescence microscopy revealed distinct eGFP protein expression patterns: D plasmid-injected embryos showed widespread expression (eyes, forebrain, spinal cord), while T plasmid-injected embryos exhibited primarily ocular expression (Figure 1F). Control embryos injected with promoter-deleted pCS2^{+}-eGFP showed no detectable fluorescence. These results demonstrate that increased *runx2b* promoter methylation in pCS2-prunx2b-eGFP can significantly reduce eGFP mRNA levels, consequently diminishing eGFP protein levels and restricting its spatial distribution. This suggests that elevating *runx2b* promoter methylation via DNA methylation tools may similarly suppress *runx2b* expression levels in zebrafish, potentially reducing related protein production and inducing phenotypic alterations.

IB length reduction through *runx2b* promoter methylation in F0

To investigate whether targeted methylation of the *runx2b* promoter can reduce *runx2b* expression levels and alter the IB phenotype, we employed the CRISPR/dCas9-Dnmt7 system in zebrafish (Liang et al., 2023a). We targeted the *runx2b* promoter in zebrafish using the

Science Press ZR Zoological Research

CRISPR/dCas9-Dnmt7 system for DNA methylation. Two sgRNAs were designed to target the CpG islands at positions -268 bp (g1) and -419 bp (g2) upstream of the *runx2b* start codon (Figure 2A; Supplementary Figure S3). At 48 hpf, RT-qPCR revealed significantly reduced *runx2b* mRNA expression levels across all experimental groups (g1, g2, g1+g2 groups; Figure 2B), confirming effective transcriptional regulation by both sgRNAs. The g1 and g1+g2 groups showed stronger suppression than g2 alone. No significant difference in *runx2b* inhibition was observed between the g1 and g1+g2 groups, with marginally lower expression in g1, suggesting that there was no synergistic effect from dual targeting. Diminished *runx2b* expression levels in the g1 embryos were further corroborated by whole-mount ISH at 48 hpf (Supplementary Figure S4). Surprisingly, sustained *runx2b* suppression in the tail muscle (0.4-fold vs. controls; Figure 2C) confirmed transcriptional inhibition during the peak IB developmental stage at 40 dpf (Yao et al., 2015). We further analyzed the methylation levels within the *runx2b* CpG island (Figure 2D), and found that the average promoter methylation level in the F0 generation zebrafish was significantly elevated compared with controls at 48 hpf (Figure 2E), confirming efficient targeted methylation by the CRISPR/dCas9-Dnmt7 system. While most individual CpG sites showed marginally increased methylation, these differences were not statistically significant (Figure 2F). To assess the phenotypic consequences, g1 group embryos were reared to adulthood. Alizarin Red S staining revealed that the IB lengths on both sides of the epineural bones in the 11^{th}-16^{th} muscle segments were significantly shorter, decreasing by 26.9%, 38.8%, 35.8%, 38.1%, 34.4%, and 23.3%, respectively (Figure 2G, H). However, the number of IBs remained almost unchanged (Figure 2I). This suggests that targeted methylation of the *runx2b* promoter via CRISPR/dCas9-Dnmt7 significantly reduces *runx2b* expression and shortens IB length without altering IB number in F0.

The *runx2b* promoter methylation-induced effects were retained in offspring

To investigate the heritable effects of *runx2b* promoter methylation on gene expression and IB phenotypes in zebrafish, we incrossed the F0 strains (g1, g2, and g1+g2 groups) to generate the F1 generation. At 48 hpf, the F1 embryos exhibited significantly reduced *runx2b* mRNA expression levels (Figure 3A). Consistent with the trends observed in F0, the g1 group showed the strongest suppression (0.16-fold), followed by the g1+g2 (0.36-fold) and g2 (0.59-fold) groups. Given its

Science Press ZR Zoological Research

maximal efficacy, we selected the g1 lineage to produce F2 offspring. The F2 strains similarly showed significant *runx2b* downregulation at 48 hpf (Figure 3B). And the corresponding protein levels decreased in all generations at 5 dpf (Supplementary Figure S5). Furthermore, whole-mount ISH results at 48 hpf confirmed that *runx2b* expression was restricted to the eyes, ethmoid plate, and pharyngeal arches in both F1 and F2, with reduced signal compared with the controls (Figure 3C). Relative *runx2b* suppression persisted at 40 dpf (Figure 3D).

DNA methylation analysis revealed hypermethylation at most sites in F1, with significant increases at nine positions located at -696 bp, -677 bp, -584 bp, -579 bp, -568 bp, -537 bp, -531 bp, -511 bp, and-77 bp (Figure 3E), which led to significantly elevated average *runx2b* promoter methylation levels in F1/F2 without an incremental trend (Figure 3F). While most sites also showed increased methylation levels in F2, with significant elevation at -584 bp and -537 bp, the increase was less pronounced compared with F1 (Figure 3E). Alizarin Red S staining of adult F1 and F2 revealed normal skeletal development, but significantly shortened epineural bones in the 11^{th}-16^{th} muscle segments, with a 17.5% to 38.0% reduction in F1 and 11.9% to 26.5% reduction in F2 (Figure 3G; Supplementary Figure S6). The IB counts remained unchanged (Supplementary Figure S7). Collectively, these results demonstrate stable transgenerational inheritance of CRISPR/dCas9-Dnmt7-induced *runx2b* suppression and the associated IB shortening without incremental methylation accumulation.

Variable IB reduction across *runx2b* knockout strains

To directly compare the functional consequences of epigenetic *runx2b* suppression versus conventional genetic knockout, we established three distinct homozygous *runx2b* knockout strains using CRISPR/Cas9. These strains harbored varied second-exon mutations: a 2-bp deletion (-2 bp), 1-bp insertion (+1 bp), and 7-bp insertion (+7 bp) (Figure 4A; Supplementary Figure S8). All mutations induced frameshifts that introduced premature stop codons, yielding truncated proteins of 106 aa (-2 bp), 107 aa (+1 bp), and 109 aa (+7 bp), representing ~370 aa truncations relative to wild-type Runx2b (477 aa). SWISS-MODEL predictions revealed substantial structural deviations from the wild-type protein, though notably, the +1 bp and +7 bp mutants exhibited similar folding patterns (Figure 4B). Alizarin Red S staining demonstrated partial-to-complete IB loss in *runx2b* mutants

Science Press
ZR Zoological Research

despite normal overall skeletal morphology (Figure 4C). Quantitative analysis revealed significantly reduced IB counts across all homozygous *runx2b* mutants, with mean values of 64.33 (-2 bp), 46 (+1 bp), and complete absence (+7 bp) (Figure 4D). These results demonstrate that IB elimination was not universally achieved across all *runx2b* knockout strains, revealing inherent mutational heterogeneity in genetically modified lines.

Transcriptome analysis of methylation-edited strains across generations

To elucidate how *runx2b* promoter methylation can regulate gene expression and IB phenotypes during development, we performed RNA-seq on tail muscle samples from 40-dpf zebrafish across generations: wild-type (CTL) and methylation-modified strains (F0, F1, F2). Differential expression analysis using DESeq2 revealed progressively increasing DEGs in successive generations (Figure 5A; Supplementary Figure S9). Venn analysis identified 40 conserved DEGs across all methylated generations (Figure 5B). Hierarchical clustering of these shared DEGs showed pronounced expression divergence from the controls, which intensified in later generations (Figure 5C). Biological replicates demonstrated consistent expression profiles, confirming data robustness.

KEGG pathway analysis revealed a consistent disruption of skeletal development across generations, with peak enrichment in F1, such as the FoxO and peroxisome proliferator-activated receptor (PPAR) signaling pathways (Figure 5D). GO analysis of the conserved DEGs across the F0, F1, and F2 methylation-modified strains identified 59 shared enriched terms (Supplementary Figure S10), with predominant involvement in intracellular signaling (Biological Process), ubiquitin ligase/transferase and glycosyltransferase activities (Molecular Function), and collagen-containing extracellular matrix (Cellular Component). Collectively, these findings demonstrate that CRISPR/dCas9-Dnmt7-mediated *runx2b* promoter methylation can disrupt skeletal development-associated mechanisms by altering ubiquitin ligase and glycosyltransferase-regulated gene expression pathways in zebrafish.

DISCUSSION

Promoter methylation represents a conserved epigenetic mechanism for gene regulation, typically silencing transcription through impaired transcription factor binding and chromatin

307 remodeling (Bouyahya et al., 2022). Numerous studies have demonstrated a significant negative
308 correlation between promoter methylation and gene expression levels. For example, in colorectal,
309 breast, and lung carcinomas, tumor suppressor genes are frequently hypermethylated, leading to
310 transcriptional silencing (Barrett et al., 2022). However, in rare cases, promoter methylation may
311 paradoxically enhance gene expression patterns, a phenomenon termed paradoxical gene activation
312 (Smith et al., 2020). The *runx2b* belongs to the *runx* family and is an ortholog of *runx2* (Pinto et al.,
313 2005). Prior to the present work, *runx2b* promoter methylation had only been correlated with
314 reduced expression levels in human osteoarthritis (Takahashi et al., 2017), with no evidence in
315 teleost. Under natural physiological conditions, elevated *runx2b* promoter methylation inhibits
316 transcription and suppresses protein expression in zebrafish, as validated by *in vivo* recombinant
317 plasmid assays (Figure 1). To investigate this mechanism, we targeted the zebrafish *runx2b* promoter
318 using a CRISPR/dCas9-Dnmt7 fusion system for site-specific methylation. Subsequent RT-qPCR
319 and whole-mount ISH experiments revealed significantly reduced *runx2b* mRNA expression levels
320 and altered spatial distribution patterns.

321 Previous studies have demonstrated that epigenetic interventions applied to the F0 generation
322 may increase instability and stochasticity due to heightened sensitivity during early development,
323 potentially preventing complete transmission to the F1 and F2 generations (Lecoutre et al., 2019).
324 To assess the heritability potential of DNA methylation-induced *runx2b* suppression, we quantified
325 methylation levels and gene expression patterns in the F0, F1, and F2 generations. Our results
326 demonstrated direct and transgenerational heritability of this epigenetic silencing mechanism in
327 zebrafish. In F0 adults, we observed significantly shortened epineural bones in the 11^{th}-16^{th} muscle
328 segments, representing the successful induction of IB abnormalities in fish via epigenome editing.
329 This aberrant phenotype persisted in both F1 and F2 offspring, confirming transgenerational
330 inheritance of methylation-mediated *runx2b* silencing. This approach provides a novel foundational
331 technology for aquatic animal breeding (Figure 5E). Notably, no dose-dependent relationship was
332 observed between *runx2b* promoter methylation levels and IB shortening, likely because wild-type
333 zebrafish exhibit > 85% baseline methylation at most promoter sites (Figure 2E, F), limiting further
334 modification potential. Unlike mammals and medaka, the global genomic methylation in zebrafish

Science Press ZR Zoological Research

stays at a high level across the lifetime without a dramatic reprogramming process, neither in early stage embryo, nor in primordial germ cell specification (Jiang et al., 2013; Ortega-Recalde et al., 2019). The underpinning mechanism and contribution of DNA methylation in gene expression regulation should be thoroughly studied. Therefore, future studies should investigate dose-response dynamics using gene promoters with lower baseline methylation patterns. In addition to DNA methylation, histone modifications are also important forms of epigenetics. Studies have reported that histone modification editing can regulate the expression of target genes (Fukushima et al., 2019). Therefore, combining DNA methylation editing with histone modification editing will be a key focus of future research.

Previous studies have demonstrated that Runx2 is essential for osteoblast differentiation and skeletal formation, functioning not only as an upstream transcriptional regulator of the osteoblast-specific transcription factor *sp*7, but also as a key modulator of bone-related signaling pathways, including the BMP, Wnt, Hedgehog, Notch, and MAPK pathways (Jonason et al., 2009). Crucially, zebrafish IB development relies on TGF-β/BMP-mediated osteoblast differentiation from tendon progenitor cells (Nie et al., 2022). In osteoblasts, the Wnt/β-catenin signaling pathway enhances the expression of osteogenic genes, such as *Runx*2, which facilitates osteoblast differentiation and bone formation (Gao et al., 2023). To elucidate the transgenerational mechanism by which *runx2b* promoter methylation can suppress IB development in zebrafish, we performed a comparative transcriptomic analysis across F0, F1, F2, and the wild-type controls. The methylated strains exhibited progressively increasing numbers of DEGs over generations. KEGG analysis revealed consistent enrichment of the PPAR and FoxO signaling pathways in all three generations. In bone marrow mesenchymal stem cells, PPARγ activation modulates osteoblast differentiation and bone formation (Akune et al., 2004). Furthermore, the FoxO signaling pathway, another commonly enriched pathway, regulates bone formation through FoxO transcription factors by suppressing PPARc, modulating osteogenic markers and osteocalcin, and interacting with the Wnt/β-catenin pathway (Siqueira et al., 2011). Therefore, we propose that zebrafish *runx2b* promoter methylation can suppress osteogenesis via PPAR/FoxO-mediated inhibition of osteogenic gene expression, culminating in aberrant IB development through impaired osteoblast proliferation.

Science Press ZR Zoological Research

Epigenetic regulation, which encompasses DNA methylation, histone modifications, and non-coding RNAs, synergistically modulates gene expression across transcriptional, chromatin, and post-transcriptional tiers (Tao et al., 2015). GO analysis revealed that the DEGs were enriched in various molecular functions, such as ubiquitin-protein ligase activity and ubiquitin-protein transferase activity, as well as cellular components, like the collagen-containing extracellular matrix. Ubiquitin-protein ligases and transferases primarily participate in histone ubiquitination (Liselot et al., 2024), while the collagen-rich extracellular matrix interacts with osteoblasts to promote their proliferation and differentiation (Jacobson et al., 2024). These enriched GO terms suggest that *runx2b* promoter methylation may synergistically induce histone ubiquitination modifications, contributing to runx2b protein degradation, collectively suppressing osteogenesis and abrogating IB development.

CRISPR/Cas9-mediated *runx2b* knockout generated three homozygous mutant strains. Adult zebrafish exhibited distinct IB phenotypes, in which the -2 bp mutant had an average IB reduction of 23.7%, the +1 bp mutant had a 45.4% reduction in the IB number, and the +7 bp mutant exhibited complete IB loss. These findings indicate that different zebrafish *runx2b* mutant types have varying IB growth conditions. Notably, *runx2b* promoter methylation attenuated, but did not abolish, IB formation, contrasting with knockout efficacy. This attenuated methylation efficacy relative to knockout arises from two mechanistic constraints: 1) wild-type zebrafish exhibit a high baseline methylation at *runx2b* promoter CpG sites, minimizing further suppression potential, and 2) methylation partially represses *runx2b* expression levels, permitting residual Runx2b protein production, whereas knockout ablates the functional protein via frameshift mutations. Because *runx2b* is indispensable for IB morphogenesis, complete protein elimination underpins the superior efficacy of the knockout. However, there are still many unanswered questions regarding the epigenetic regulatory mechanisms. For instance, it remains unclear which sites are the key sites required for methylation regulation. Therefore, several issues require further investigation: first, the identification and analysis of key epigenetic regulatory elements in the genome; second, exploring the interplay between genome-wide methylation modifications and histone modifications, which requires further study.

Science Press ZR Zoological Research

CONCLUSION

In summary, our study represents the application of the CRISPR/dCas9-Dnmt7-mediated promoter methylation editing technology to suppress expression of *runx2b*, a key gene regulating IB development, thereby affecting its normal growth. Notably, the inhibitory effects were shown to be direct and transgenerational heritable. Mechanistically, *runx2b* promoter hypermethylation can initiate transcriptional silencing, compounded by histone ubiquitination-mediated Runx2b degradation and PPAR/FoxO-dependent inhibition of osteoblast proliferation/differentiation, ultimately impairing normal IB development. By leveraging such epigenetic modifications for trait engineering, we have established a safer, adaptable genome-editing paradigm with transformative potential for aquaculture breeding.

DATA AVAILABILITY

The raw sequence data reported in this paper have been deposited in the Genome Sequence Archive (Zhang et al., 2025) in National Genomics Data Center(Members & Partners, 2024) (accessible at https://ngdc.cncb.ac.cn/gsa), under accession numbers: CRA033575 for RNA-seq and CRA033601 for Multiplex Bisulfite Sequencing.

CONFLICT OF INTEREST

The authors declare that they have no competing interests.

AUTHOR CONTRIBUTION

Fang Liang: Conceptualization, Investigation, Formal analysis, Writing – original draft, and Funding Acquisition; **Biyu Wu:** Investigation, Formal analysis and Writing – original draft; **Jiayi Liu:** Investigation, Formal analysis; **Xue Wang:** Methodology, Investigation; **Minxing Liang**: Investigation; **Chaoyi Wang**: Investigation, Formal analysis; **Jingyi Zhang**: Conceptualization, Investigation; **Junjie Wang**: Resources, Methodology; **Yutao Miao**: Resources; **Kangsen Mai**: Resources, Conceptualization, Supervision; **Jun Zhao**: Supervision, Methodology, Resources;

Science Press ZR Zoological Research

Xuegeng Wang: Conceptualization, Funding Acquisition, Supervision, Writing – review & editing. All authors read and approved the final version of the manuscript.

ACKNOWLEDGMENTS

Authors would like to acknowledge the colleagues of School of Life Sciences, South China Normal University for their technical assistance. We thank J. Iacona, Ph.D., from Liwen Bianji (Edanz) for editing the English text of a draft of this manuscript.

FUNDING

This work was supported by the National Natural Science Foundation of China (22176066 to X. W., 32300692 to F. L.), China Postdoctoral Science Foundation (2024T170292 to F.L.), the Guangdong Basic and Applied Basic Research Foundation (2025A1515012118 to F.L.), the Guangzhou Science Program (2025A04J3596 to X. W.).

REFERENCES

Akune T, Ohba S, Kamekura S, et al. 2004. PPARγ insufficiency enhances osteogenesis through osteoblast formation from bone marrow progenitors. *Journal of Clinical Investigation*, **113**(6): 846-855.

Allis CD & Jenuwein T. 2016. The molecular hallmarks of epigenetic control. *Nature Reviews Genetics*, **17**(8): 487-500.

Barrett JE, Herzog C, Jones A, et al. 2022. The WID-BC-index identifies women with primary poor prognostic breast cancer based on DNA methylation in cervical samples. *Nature Communications*, **13**(1): 449-449.

Bouyahya A, Mechchate H, Oumeslakht L, et al. 2022. The Role of Epigenetic Modifications in Human Cancers and the Use of Natural Compounds as Epidrugs: Mechanistic Pathways and Pharmacodynamic Actions. *Biomolecules*, **12**(3): 367.

Chen S, Zhou Y, Chen Y, et al. 2018. fastp: an ultra-fast all-in-one FASTQ preprocessor. *Bioinformatics*, **34**(17): i884-i890.

Chitramuthu BP & Bennett HPJ. 2013. High Resolution Whole Mount *In Situ* Hybridization within Zebrafish Embryos to Study Gene Expression and Function. *Jove-Journal of Visualized Experiments*, **80**: e50644.

Concordet J-P & Haeussler M. 2018. CRISPOR: intuitive guide selection for CRISPR/Cas9 genome editing experiments and screens. *Nucleic Acids Research*, **46**(W1): W242-W245.

Science Press ZR Zoological Research

Consortium GO. 2015. Gene ontology consortium: going forward. *Nucleic Acids Research*, **43**(D1): D1049-D1056.

Danos N & Ward AB. 2012. The homology and origins of intermuscular bones in fishes: phylogenetic or biomechanical determinants. *Biological Journal of the Linnean Society*, **106**(3): 607-622.

Dong Q, Nie CH, Wu YM, et al. 2023. Generation of blunt snout bream without intermuscular bones by runx2b gene mutation. *Aquaculture*, **567**: 739263.

Erik S. 2020. Tomorrow's catch. *Science (New York, N.Y.)*, **370**(6519): 902-905.

Flores MV, Tsang VW, Hu W, et al. 2004. Duplicate zebrafish runx2 orthologues are expressed in developing skeletal elements. *Gene Expr Patterns*, **4**(5): 573-581.

Fukushima HS, Takeda H, Nakamura R. 2019. Targeted in vivo epigenome editing of H3K27me3. *Epigenetics & Chromatin*, **12**(1): 17.

Gan RH, Li Z, Wang ZW, et al. 2023. Creation of intermuscular bone-free mutants in amphitriploid gibel carp by editing two duplicated *runx2b* homeologs. *Aquaculture*, **567**: 739300.

Gao YG, Chen N, Fu ZD, et al. 2023. Progress of Wnt Signaling Pathway in Osteoporosis. *Biomolecules*, **13**(3): 483.

Harvey ZH, Chen Y, Jarosz DF. 2018. Protein-Based Inheritance: Epigenetics beyond the Chromosome. *Molecular Cell*, **69**(2): 195-202.

Jacobson KR, Saleh AM, Lipp SN, et al. 2024. Extracellular matrix protein composition dynamically changes during murine forelimb development. *iScience*, **27**(2): 108838.

Jiang L, Zhang J, Wang J-J, et al. 2013. Sperm, but not oocyte, DNA methylome is inherited by zebrafish early embryos. *Cell*, **153**(4): 773-784.

Jin BL, Li YJ, Robertson KD. 2011. DNA methylation: superior or subordinate in the epigenetic hierarchy. *Genes & cancer*, **2**(6): 607-617.

Jonason JH, Xiao G, Zhang M, et al. 2009. Post-translational Regulation of Runx2 in Bone and Cartilage. *Journal of Dental Research*, **88**(8): 693-703.

Kim D, Langmead B, Salzberg SL. 2015. HISAT: a fast spliced aligner with low memory requirements. *Nature Methods*, **12**(4): 357-360.

Kuang YY, Zheng XH, Cao DC, et al. 2023. Generate a new crucian carp (*Carassius auratus*) strain without intermuscular bones by knocking out *bmp6*. *Aquaculture*, **569**: 1-31.

Lecoutre S, Kwok KHM, Petrus P, et al. 2019. Epigenetic Programming of Adipose Tissue in the Progeny of Obese Dams. *Current Genomics*, **20**(6): 428-437.

Li BY, Huang YS, Pi D, et al. 2024. Effects of Acute and Developmental Exposure to Bisphenol S on Chinese Medaka

Science Press
ZR Zoological Research

(*Oryzias sinensis*). *Journal of Xenobiotics*, **14**(2): 452-466.

Liang F, Dong ZJ, Ye JM, et al. 2023a. *In vivo* DNA methylation editing in zebrafish. *Epigenetics*, **18**(1): 2192326.

Liang ZY, Guo YF, Pi D, et al. 2023b. Transcriptome Analysis of the Developmental Effects of Bisphenol F Exposure in Chinese Medaka (*Oryzias sinensis*). *International Journal of Molecular Sciences*, **24**(13): 10898.

Liselot VL, Nicky TV, Mannens MM, et al. 2024. Molecular signatures in Mendelian neurodevelopment: a focus on ubiquitination driven DNA methylation aberrations. *Frontiers in Molecular Neuroscience*, **17**: 1446686.

Liu XS, Wu H, Krzisch M, et al. 2018. Rescue of Fragile X Syndrome Neurons by DNA Methylation Editing of the FMR1 Gene. *Cell*, **172**(5): 979-992.e976.

Love MI, Huber W, Anders S. 2014. Moderated estimation of fold change and dispersion for RNA-seq data with DESeq2. *Genome biology*, **15**(12): 550.

Members C-N & Partners. 2024. Database Resources of the National Genomics Data Center, China National Center for Bioinformation in 2025. *Nucleic Acids Research*, **53**(D1): D30-D44.

Nie CH, Wan SM, Chen YL, et al. 2022. Single-cell transcriptomes and *runx2b*$^{-/-}$ mutants reveal the genetic signatures of intermuscular bone formation in zebrafish. *National Science Review*, **9**(11): 1-21.

Nilsson E, Sadler-Riggleman I, Beck D, et al. 2021. Differential DNA methylation in somatic and sperm cells of hatchery vs wild (natural-origin) steelhead trout populations. *Environmental Epigenetics*, **7**(1): dvab002.

Okoli AS, Blix T, Myhr AI, et al. 2022. Sustainable use of CRISPR/Cas in fish aquaculture: the biosafety perspective. *Transgenic Research*, **31**(1): 1-21.

Ortega-Recalde O, Day RC, Gemmell NJ, et al. 2019. Zebrafish preserve global germline DNA methylation while sex-linked rDNA is amplified and demethylated during feminisation. *Nature Communications*, **10**(1): 3053.

Park H, Shin J, Kim Y, et al. 2022. CRISPR/dCas9-Dnmt3a-mediated targeted DNA methylation of *APP* rescues brain pathology in a mouse model of Alzheimer's disease. *Translational Neurodegeneration*, **11**(1): 41-53.

Pinto JP, Conceiçao NM, Viegas CS, et al. 2005. Identification of a new pebp2αA2 isoform from zebrafish *runx*2 capable of inducing osteocalcin gene expression in vitro. *Journal of Bone and Mineral Research*, **20**(8): 1440-1453.

Podgorniak T, Dhanasiri A, Chen X, et al. 2022. Early fish domestication affects methylation of key genes involved in the rapid onset of the farmed phenotype. *Epigenetics*, **17**(10): 1281-1298.

Sadakierska-Chudy A, Kostrzewa RM, Filip M. 2015. A Comprehensive View of the Epigenetic Landscape Part I: DNA Methylation, Passive and Active DNA Demethylation Pathways and Histone Variants. *Neurotoxicity Research*, **27**(1): 84-97.

Siqueira MF, Flowers S, Bhattacharya R, et al. 2011. FOXO1 modulates osteoblast differentiation. *BONE*, **48**(5): 1043-1051.

Science Press
ZR Zoological Research

509 Smith J, Sen S, Weeks RJ, et al. 2020. Promoter DNA Hypermethylation and Paradoxical Gene Activation. *Trends in*
510 *Cancer*, **6**(5): 392-406.

511 Takahashi A, De AMC, Hashimoto K, et al. 2017. DNA methylation of the RUNX2 P1 promoter mediates MMP13
512 transcription in chondrocytes. *Scientific reports*, **7**(1-4): 7771.

513 Tao LC, Bei YH, Zhou YL, et al. 2015. Non-coding RNAs in cardiac regeneration. *Oncotarget*, **6**(40): 42613-42622.

514 Thisse C & Thisse B. 2008. High-resolution *in situ* hybridization to whole-mount zebrafish embryos. *Nature Protocols*,
515 **3**(1): 59-69.

516 Wang X, Bhandari RK, Mai K. 2024. Epigenome editing: A new approach to aquaculture breeding. *Reviews in*
517 *Aquaculture*, **16**(4): 1463-1466.

518 Xu H, Tong GX, Yan T, et al. 2022. Transcriptomic Analysis Provides Insights to Reveal the *bmp*6 Function Related to
519 the Development of Intermuscular Bones in Zebrafish. *Frontiers in Cell and Developmental Biology*, **10**: 821471.

520 Yao W, Lv Y, Gong X, et al. 2015. Different ossification patterns of intermuscular bones in fish with different swimming
521 modes. *Biol Open*, **4**(12): 1727-1732.

522 Yuta T, Mariana MV, Yang Y, et al. 2023. Transgenerational inheritance of acquired epigenetic signatures at CpG islands
523 in mice. *Cell*, **186**(4): 715-731.

524 Zhang S, Chen X, Jin E, et al. 2025. The GSA Family in 2025: A Broadened Sharing Platform for Multi-omics and
525 Multimodal Data. *Genomics, Proteomics & Bioinformatics*, **23**(4).

526 Zhong ZH, Feng SH, Duttke SH, et al. 2021. DNA methylation-linked chromatin accessibility affects genomic
527 architecture in *Arabidopsis*. *Proceedings of the National Academy of Sciences of The United States of America*, **118**(5):
528 1-10.

529

530

Science Press
ZR Zoological Research

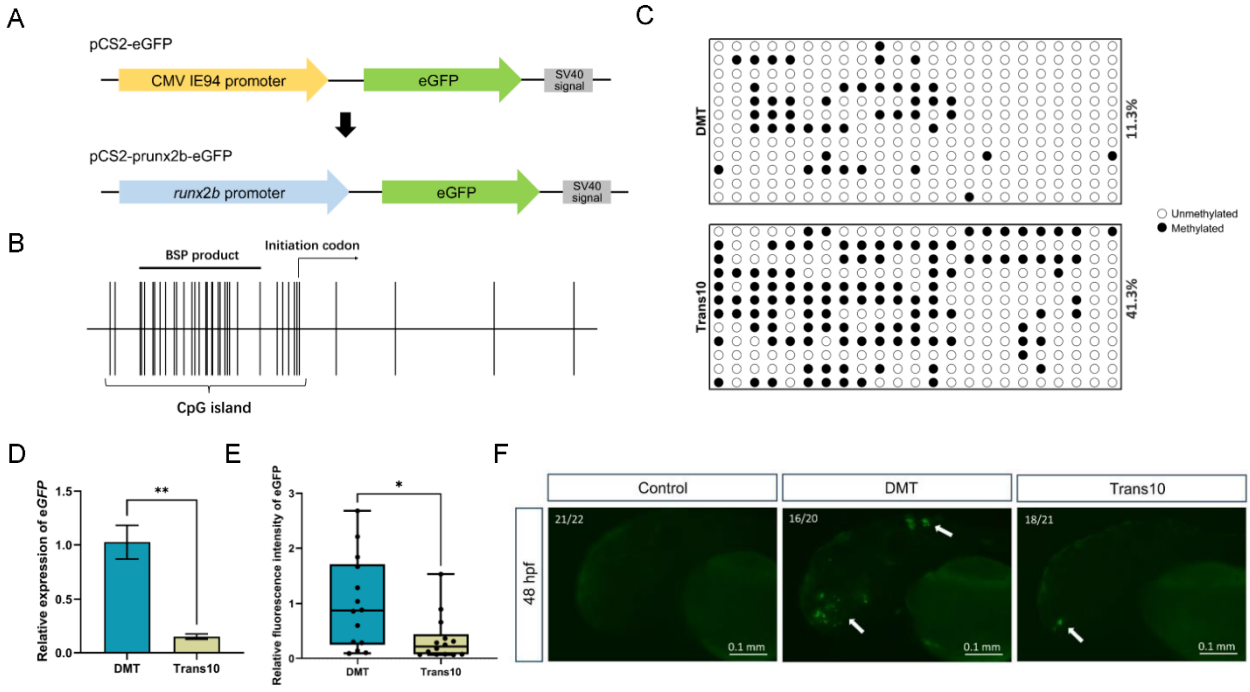

Figure 1 Increased methylation of the *runx2b* promoter suppresses eGFP expression in zebrafish. (A) Construction of the pCS2^{+}-prunx2b-eGFP plasmid. (B) Schematic of CpG sites within the *runx2b* promoter. (C) Changes in *runx2b* promoter methylation levels induced by transformation into different competent cells. Each sample represents a pooled clone analyzed by bisulfite sequencing PCR (BSP), with 12 replicates shown; each row of circles depicts the methylation status from one BSP clone. (D) Relative expression of *eGFP* mRNA at 48 hpf in zebrafish. (E) Relative eGFP fluorescence intensity at 48 hpf in zebrafish. (F) Expression of eGFP fluorescent protein in zebrafish embryos following injection of different plasmids. The white arrows indicate sites of eGFP expression; scale bar = 0.1 mm. *$P < 0.05$, **$P < 0.01$

Science Press
ZR Zoological Research

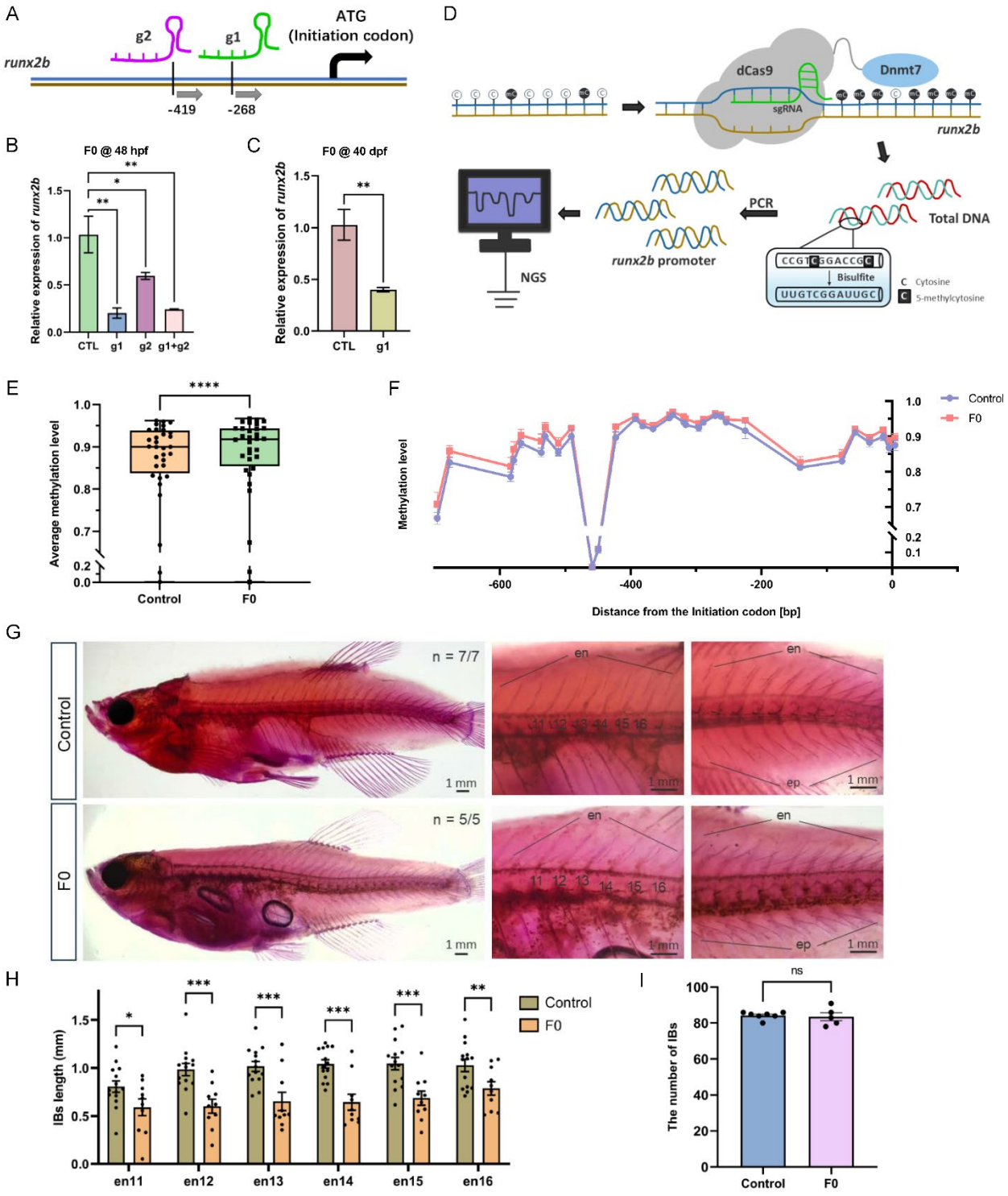

Figure 2 dCas9-Dnmt7 mediated methylation of the *runx2b* promoter *in vivo*. (A) Schematic of the relative positions of *runx2b* promoter-targeting single guide RNAs (sgRNAs). (B), (C) Relative *runx2b* expression levels in the F0 generation at 48 hpf and 40 dpf. (D) Workflow for DNA methylation level analysis in this study. (E) Average methylation level of the *runx2b* promoter following targeted methylation; ****$P < 0.0001$. (F) Methylation levels at individual CpG sites within the *runx2b* promoter. (G) Alizarin Red S staining pattern in the

Science Press
ZR Zoological Research

F0 generation; en: epineural bone, ep: epipleural bone, scale bar = 1 mm. (H) Length of epineural bones in the 11th-16th muscle segments of the F0 generation. (I) Number of IBs in the F0 generation; $P > 0.05$ (ns). *$P < 0.05$, **$P < 0.01$, ***$P < 0.001$.

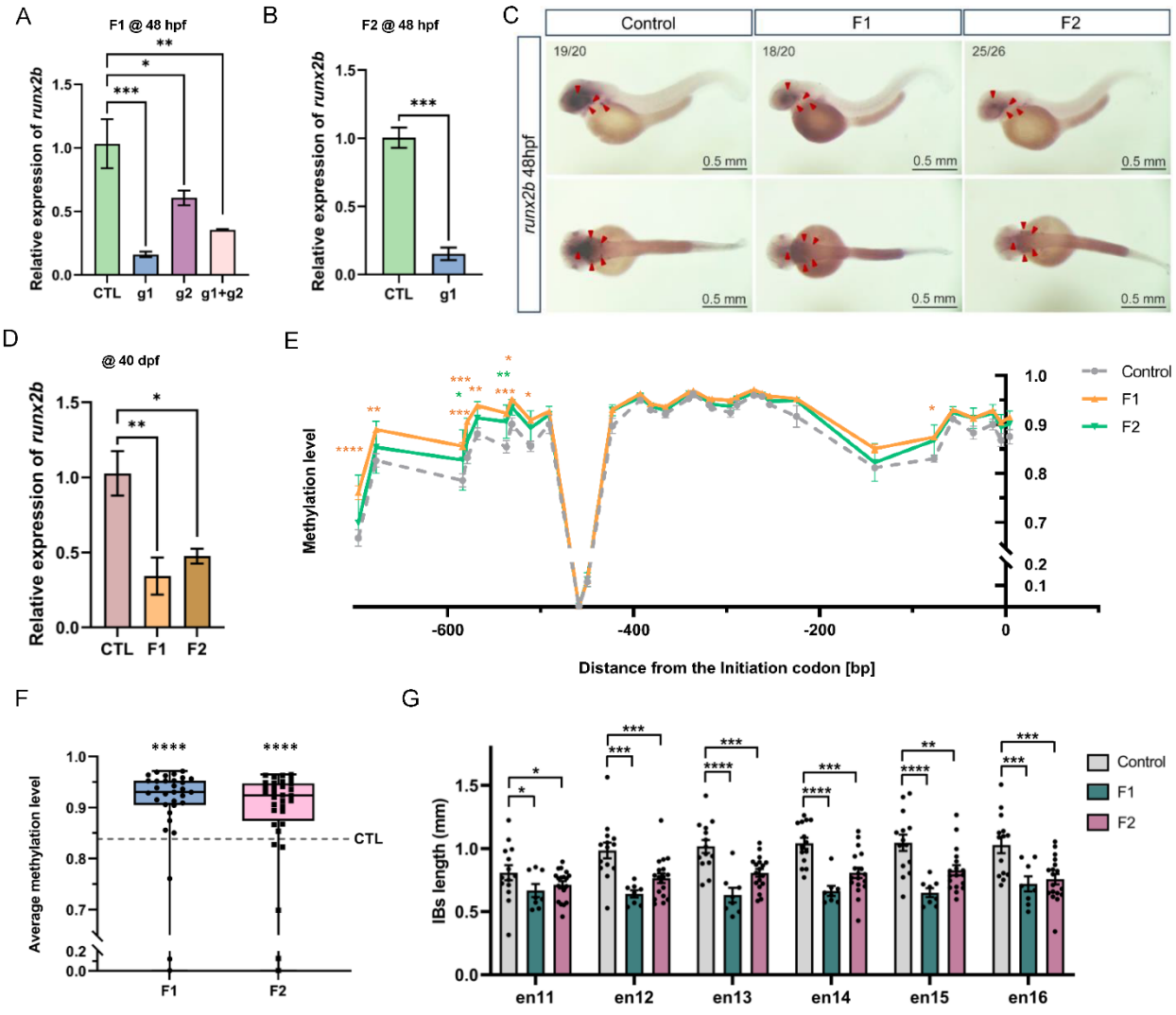

Figure 3 Heritable effects of *runx2b* promoter methylation. (A), (B) Relative *runx2b* expression at 48 hpf in the F1 generation (A) and F2 generation (B). (C) Whole-mount *in situ* hybridization of *runx2b* in offspring embryos at 48 hpf. The red arrows indicate *runx2b* mRNA expression sites; scale bar = 0.5 mm. (D) Relative *runx2b* expression in *runx2b* promoter methylation-edited offspring at 40 dpf. (E) Methylation levels at individual CpG sites in the offspring. (F) Average *runx2b* promoter methylation in the offspring. The gray dashed line indicates wild-type average methylation. (G) IB length in the 11th-16th muscle segments of the F1 and F2 generations. $P > 0.05$ (ns) *$P < 0.05$, **$P < 0.01$, ***$P < 0.001$, ****$P < 0.0001$.

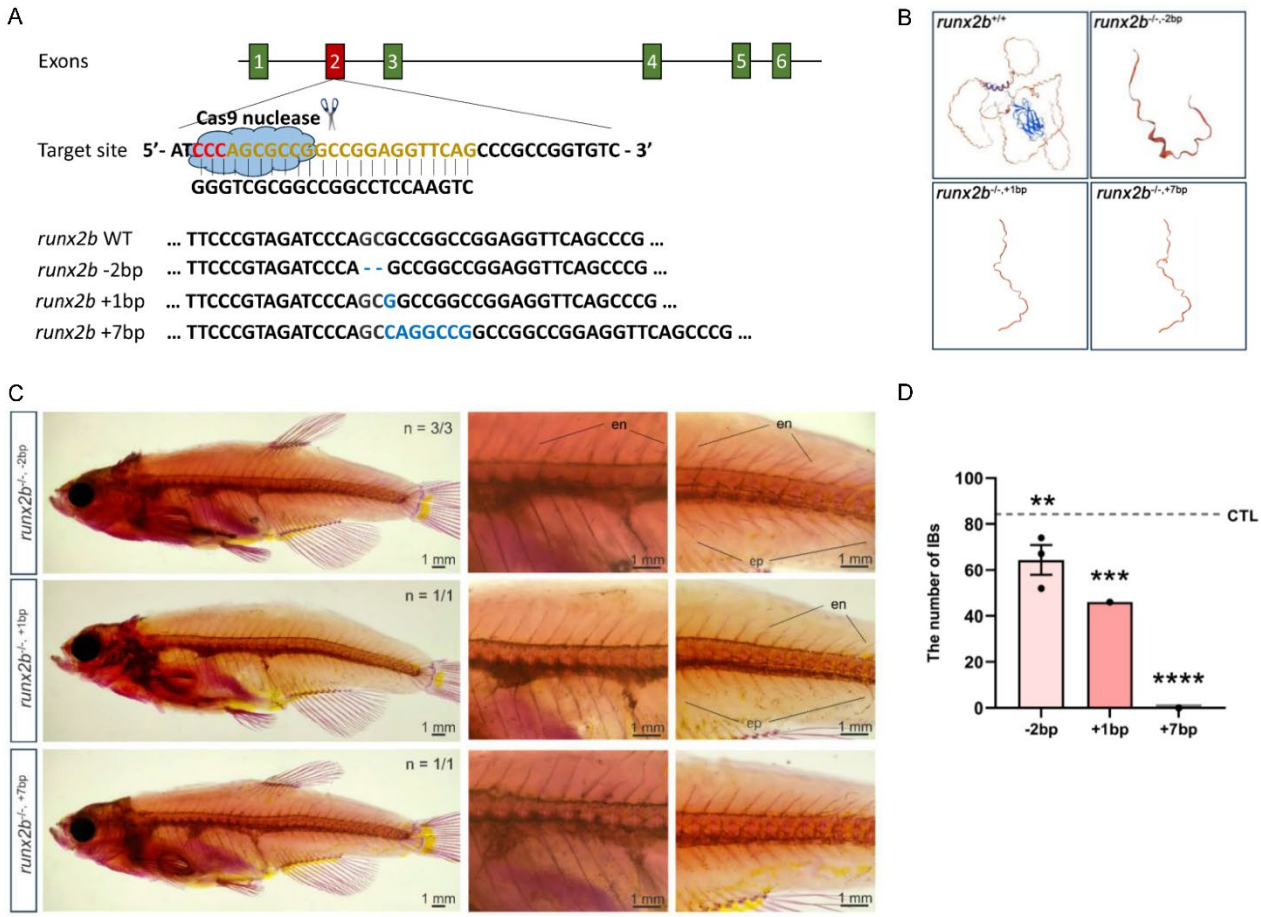

Figure 4 Reduced intermuscular bone (IB) count in homozygous *runx2b* knockout mutants. (A) Illustration describing the target sequence and predicted protein sequences based on the DNA sequence in wild-type and *runx2b*$^{-/-}$ mutants. (B) Predicted protein structure of the *runx2b* knockout mutants. (C) IB phenotypes of the *runx2b* knockout mutants. (D) Number of IBs in the *runx2b* knockout mutants; $^{**}P < 0.01$, $^{***}P < 0.001$, $^{****}P < 0.0001$; en: epineural bone, ep: epipleural bone. Note: The dorsal fin of the +1 bp mutant was lost during staining.

Science Press
ZR Zoological Research

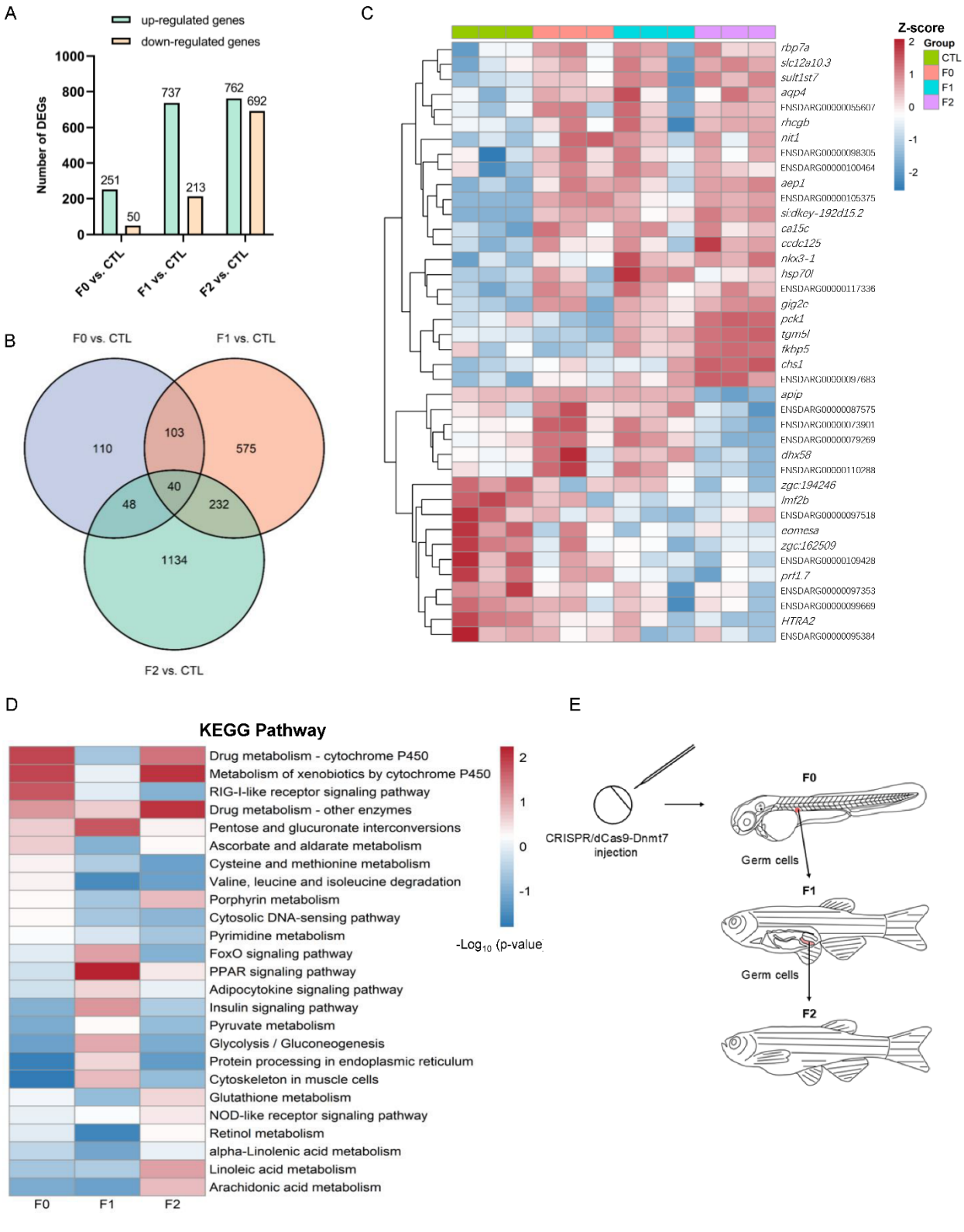

Figure 5 Transcriptomic profiling of differentially expressed genes (DEGs) in *runx2b*-methylated lineages across generations. (A) Column charts showing the number of DEGs per generation. Thresholds: $|\log_2 FC| > 1$, *P*-value < 0.05. (B) Venn diagram of generation-specific DEGs relative to the control. (C) Expression heatmap of the conserved DEGs across all generations. (D) KEGG pathways commonly enriched in the methylated generations.

574 (E) Schematic Representation of the Inheritance Patterns in Methylated Lineages Across Generations.
575

Science Press
ZR Zoological Research

斑马鱼 *runx2b* 启动子甲基化编辑获得的表观遗传标记与肌间骨减小性状的跨代遗传

梁芳 [1,2,#]，吴碧瑜 [1,#]，刘佳艺 [1]，王雪 [1]，梁敏行 [1]，汪超毅 [1]，章静宜 [1]，王俊杰 [1,2]，苗玉涛 [1,2]，麦康森 [1,3]，赵俊 [1,*]，王学耕 [1,2,*]

[1] 华南师范大学生命科学学院，现代水产养殖科学与工程研究院，粤澳水产种业发展与创新联合实验室，广东 广州 510631

[2] 华南师范大学生命科学学院，广东省昆虫发育生物学与应用技术重点实验室，广东 广州 510631

[3] 中国海洋大学水产学院，山东 青岛 266003

[#] 共同第一作者

[*] 通讯作者：赵俊 (Email: zhaojun@scnu.edu.cn)；王学耕(Email: wangxuegeng@scnu.edu.cn)

摘要：肌间骨的存在直接影响养殖鱼类的经济价值。虽然基因组编辑技术（如敲除 *runx2b* 等关键基因）能够创制无肌间骨鱼类，但其伴随的 DNA 序列改变引发了食品安全与健康担忧，从而限制了该技术在育种中的应用。本研究利用 CRISPR/dCas9 介导的表观基因组编辑技术，在不改变 DNA 序列的前提下，靶向斑马鱼 *runx2b* 启动子区域改变其 DNA 甲基化模式。结果显示，较高的 *runx2b* 启动子甲基化水平能显著抑制重组质粒中 *eGFP* mRNA 的表达。通过 CRISPR/dCas9-Dnmt7 系统提高斑马鱼 *runx2b* 启动子甲基化后，在 F0 代中观察到 *runx2b* mRNA 表达水平显著下降，成年 F0 代亲鱼第 11-16 肌节段的肌间骨长度较对照组明显缩短。通过内交获得 F1 与 F2 代子鱼，这些后代仍维持较高的启动子甲基化水平，并持续表现出 *runx2b* 表达抑制与肌间骨发育受阻。转录组测序分析表明，提高 *runx2b* 启动子甲基化水平可能协同诱发其他表观遗传修饰，潜在影响 PPAR 信号通路和 FoxO 转录因子调控，从而抑制成骨细胞的增殖与分化。综上所述，本研究展示了表观遗传编辑技术在水产育种中的创新性应用潜力。该技术可在保持基因组 DNA 完整性的前提下，精准调控重要经济性状关键基因的表达模式，为鱼类经济性状的改良提供了理论基础与技术支撑。

关键词：CRISPR/dCas9；*runx2b*；DNA 甲基化；肌间骨；斑马鱼

Science Press ZR Zoological Research